

Quantitative Imaging with Eigenfunctions of the Scattering Operator

T. Douglas Mast¹, Adrian I. Nachman², Dong-Lai Liu³, and Robert C. Waag⁴

¹Applied Research Laboratory, The Pennsylvania State University, University Park, PA 16802

²Dept. of Mathematics, University of Rochester, Rochester, NY 14627

³Siemens Medical Systems, Ultrasound Group, Issaquah, WA 98027

⁴Depts. of Electrical Engineering and Radiology, University of Rochester, Rochester, NY 14627

Abstract—An inverse scattering method that uses eigenfunctions of the scattering operator is described. This approach provides a unified framework that encompasses eigenfunction methods of focusing and quantitative image reconstruction in arbitrary media. Scattered acoustic fields are expressed using a compact, normal operator. The eigenfunctions of this operator correspond to the far-field patterns of source distributions that are directly proportional to the position-dependent contrast of a scattering object. The eigenfunctions also constitute a basis of an operator that is essentially equivalent to the time-reversal operator previously defined by others. Incident wave patterns specified by these eigenfunctions are used in a method that employs products of numerically calculated fields of the eigenfunctions to represent an unknown scattering medium. Analytic reconstruction formulas are derived both for the linearized inverse scattering problem and for the nonlinear problem in which the total acoustic pressure within the medium can be estimated. A modified eigenfunction imaging method that allows efficient reconstructions of large inhomogeneities is also presented. The methods are applied to obtain quantitative images of various scattering objects that span regions large compared to the wavelength of the acoustic illumination. The eigenfunction method is compared to the method of filtered backpropagation implemented by numerical quadrature and to Fourier inversion implemented by fast Fourier transformation. The results show the capability of the eigenfunction method to image objects with large ka . The results show the eigenfunction method is more efficient than the backpropagation method and can also be more efficient than Fourier inversion when the scattering operator has few eigenvalues.

I. INTRODUCTION

A new inverse scattering method, which employs the focusing properties of certain acoustic fields obtained by retransmitting eigenfunctions of the scattering operator, has been developed [1]. The method brings together concepts including the “power method” previously applied in electric impedance tomography [2],[3], acoustic time reversal [4]–[7], and the localized nonlinear approximation [8] to provide a general approach to quantitative ultrasonic imaging. The current paper briefly reviews the method, presents a modified eigenfunction method appropriate for reconstruction of large inhomogeneities, and shows new results including a comparison of efficiency between the eigenfunction method, filtered backpropagation, and Fourier inversion.

Funding for this work was provided by US Army Grant DAMD17-94-J-4384, the University of Rochester Diagnostic Ultrasound Research Laboratory Industrial Associates, NIH Grants DK 45533, HL 150855, and CA 74050, and ONR Grant N00014-91-1107.



Fig. 1. Scattering configuration: an incident ultrasonic wave traveling in the direction α is scattered by an inhomogeneity and the scattered far-field pressure is measured as a function of the angle θ .

II. THEORY

In the present inverse scattering method, an inhomogeneous medium is defined by the scattering potential $q(\mathbf{x}) = -k^2\gamma_\kappa(\mathbf{x})$, where k is the wavenumber $2\pi f/c$ and γ_κ is the compressibility variation [9].

The scattering configuration considered is sketched in Figure 1. For a measurement radius r in the far field, a measurement angle θ , and an incident plane wave $e^{ik\mathbf{x}\cdot\alpha}$, the far-field pattern of the scattered pressure is

$$A(\theta, \alpha) = \int e^{-ik\theta\cdot\mathbf{x}} q(\mathbf{x}) p(\mathbf{x}, \alpha) d\mathbf{x}. \quad (1)$$

This integral (like subsequent integrals on x) is two-dimensional and is taken on the entire plane in \mathbb{R}^2 .

When the incident pressure is a superposition of plane waves propagating in all directions, weighted by the complex function f , the far-field pattern of the corresponding scattered acoustic pressure is given by the operator A applied to the function f :

$$Af(\theta) = \int A(\theta, \alpha) f(\alpha) d\alpha. \quad (2)$$

The focusing properties of A are seen by considering the ratio of the scattered amplitude to the incident amplitude. Since A is normal, the magnitude of its largest eigenvalue is equal to the largest possible value of this ratio for any

nonzero f :

$$|\lambda_1| = \sup \left[\frac{\|Af(\theta)\|_{L^2}}{\|f(\theta)\|_{L^2}} \right], \quad (3)$$

where $\sup(\cdot)$ denotes the least upper bound and $\|f(\cdot)\|_{L^2}$ denotes the root-mean-square magnitude of a square-integrable function. Thus, the eigenfunction associated with the largest eigenvalue of A specifies an incident-wave distribution that maximizes the energy scattered to the far field. Other eigenfunctions also focus energy on inhomogeneities with an efficiency that is quantified by the associated eigenvalues. Notable is that analogous focusing properties also exist for the time reversal operator as defined in Ref. [7].

Because of these focusing properties, retransmitted fields of eigenfunctions are a useful starting point for inverse scattering reconstructions. The starting point for our method is an expression of the inverse scattering problem in terms of the operator A of Equation 2 and the corresponding retransmitted fields of eigenfunctions

$$\langle Af_i, f_j \rangle = \delta_{ij} \lambda_i = \int F_i(\mathbf{x}) E_j^*(\mathbf{x}) q(\mathbf{x}) dx, \quad i, j = 1, 2, \dots \quad (4)$$

$$\begin{aligned} E(\mathbf{x}) &= \int f(\alpha) e^{ik\alpha \cdot \mathbf{x}} d\alpha, \\ F(\mathbf{x}) &= \int f(\alpha) p(\mathbf{x}, \alpha) d\alpha. \end{aligned} \quad (5)$$

The problem can be regularized by seeking the solution that minimizes a weighted L^2 norm [1]. The minimization problem is then solved using the method of Lagrange multipliers, analogous to the approach used in Ref. [10] for a linearized electric impedance tomography problem. The result follows that if the potential $q_M(\mathbf{x})$ solves the regularized inverse scattering problem defined here, q_M must be of the form

$$q_M(\mathbf{x}) = \frac{1}{W(\mathbf{x})} \sum_l \sum_m Q_{lm} F_l(\mathbf{x}) \bar{F}_m^*(\mathbf{x}), \quad (6)$$

where $W(\mathbf{x})$ is an appropriate weighting function, $\bar{F}_m^*(\mathbf{x})$ is the complex conjugate of the retransmitted field corresponding to an incoming condition at infinity, and the coefficients Q_{lm} are the Lagrange multipliers.

By substituting Equation 6 into Equation 4, the inverse problem is reduced to the problem of finding the coefficients Q_{lm} from the nonlinear system

$$\delta_{ij} \lambda_i = \sum_l \sum_m \left[\int F_l(\mathbf{x}) E_j^*(\mathbf{x}) F_l(\mathbf{x}) \bar{F}_m^*(\mathbf{x}) * W(\mathbf{x})^{-1} dx \right] Q_{lm}, \quad i, j = 1, 2, \dots,$$

where the dependence of the fields F and \bar{F}^* on the scattering potential q is implicit.

In general, the scattering potential $q(\mathbf{x})$, and therefore the total pressure field $p(\mathbf{x}, \alpha)$, are unknown in inverse scattering problems. The function $p(\mathbf{x}, \alpha)$ that implicitly appears in Equation 7 may therefore be replaced by the best available estimate for the total pressure. Equation 7 can then be solved for the coefficients Q_{lm} by standard numerical techniques for solution of linear systems.

The above method simplifies further in the case of a weakly-scattering medium, for which the total pressure p can be approximated by the incident pressure. In this case, the solution is given by the coefficients

$$Q_{lm} = \frac{k^2}{8\pi^2} \iint |\sin(\theta - \alpha)| A(\theta, \alpha) f_l^*(\theta) f_m(\alpha) d\alpha d\theta. \quad (7)$$

It has been shown in Ref. [1] that this solution is analytically equivalent to the well-known filtered backpropagation algorithm for diffraction tomography under the Born approximation.

The efficiency of the eigenfunction method for large inhomogeneities can be improved by use of the eigenfunctions and eigenvalues of the operator

$$\tilde{A}(\theta, \alpha) = |\sin(\theta - \alpha)| A(\theta, \alpha). \quad (8)$$

For weak scattering, the reconstruction formula then reduces to the single summation

$$q_B(\mathbf{x}) = \sum_i \frac{k^2}{8\pi^2} \tilde{\lambda}_i |\tilde{E}_i|^2, \quad (9)$$

where $\tilde{\lambda}_i$ and \tilde{E}_i respectively are eigenvalues and retransmitted fields associated with eigenfunctions of \tilde{A} .

The eigenfunction method can also be employed for inversions that do not employ the Born approximation but maintain computational efficiency superior to alternative methods. One such application is demonstrated by considering the case where the inhomogeneous-medium retransmitted fields F can be estimated from a first approximation to the scattering potential q . We invoke the localized nonlinear approximation introduced in Ref. [8] for electromagnetic scattering. Under this approximation, the total acoustic pressure is approximated by the formula [1],[8]

$$p(\mathbf{x}, \alpha) \approx \frac{e^{ik\alpha \cdot \mathbf{x}}}{1 + \int q(\mathbf{y}) G_0(\mathbf{x} - \mathbf{y}) dy}. \quad (10)$$

The result follows that the scattering potential is approximated by the nonlinear formula

$$q_M(\mathbf{x}) \approx \sum_l \sum_m Q_{lm} (2E_l(\mathbf{x}) - F_l(\mathbf{x})) E_m^*(\mathbf{x}). \quad (11)$$

This nonlinear equation for the potential q_M can be approximately solved by using a form of the retransmitted field $F_l(\mathbf{x})$ corresponding to the lowpass-filtered potential q_B or to another estimate of the scattering potential. A similar derivation can be carried out using eigenfunctions of the operator \tilde{A} .

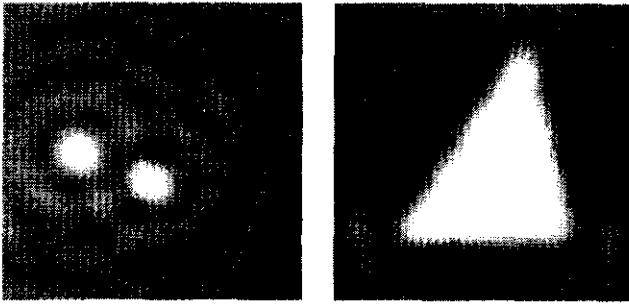


Fig. 2. Left Panel: single-frequency reconstruction of two point scatterers from scattering data with SNR of 3 dB. Right Panel: single-frequency reconstruction of a uniform triangle.

III. NUMERICAL RESULTS

Figures 2–5 show example two-dimensional reconstructions obtained with the eigenfunction methods described above. The images shown were obtained using scattering operators computed by a finite-element/Nyström method [11] as well as exact numerical solutions for scattering from penetrable cylinders [9]. These operators were sampled at 128 or 256 equally-spaced angles, so that eigenfunctions and eigenvalues of these operators could be obtained by numerical diagonalization of a 128×128 or 256×256 matrix.

Figure 2 shows high-resolution images of small structures, obtained with computational speed not possible from conventional inverse scattering techniques. The two wires shown in the first panel were obtained using only two eigenfunctions of the scattering operator, but show sub-wavelength resolution and insensitivity to noise (the signal-to-noise ratio for this image was 3 dB). The triangle shown in the second panel was reconstructed using fifteen eigenfunctions. This reconstruction required 69.1 s of cpu time on a Sun SpareStation 10, while an analogous reconstruction employing filtered backpropagation required 3014.3 s.

Example reconstructions of a large inhomogeneous object, chosen to mimic properties of tissue in medical ultrasonic imaging, are shown in Figures 3 and 4. The first panel of Figure 3 shows a quantitative image of a simulated phantom that includes a fat-mimicking background, a point-like scatterer, a cystic region, and a tumor-mimicking region. The image was obtained using the eigenfunction method for five scattering frequency components such that $20 < ka < 30$, where a is the cylinder. The second panel of Figure 3 shows a reconstruction of the same test object for scattering data corrupted by noise having a root-mean-square amplitude one-half that of the scattering data. A nonlinear reconstruction of this object, obtained using an estimate for the total pressure in the background cylinder, is presented in Figure 4. This reconstruction shows improved point resolution, seen by the increased height of the peak in the real part, and improved accuracy, seen by the overall reduction in the imaginary part.

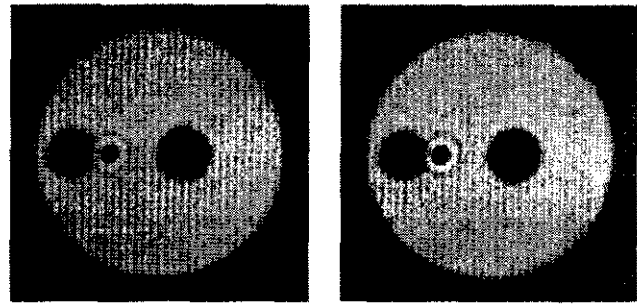


Fig. 3. Real part of imaging phantom reconstructions obtained from computed five-frequency scattering data. Left Panel: ideal data. Right Panel: data with 6 dB SNR.

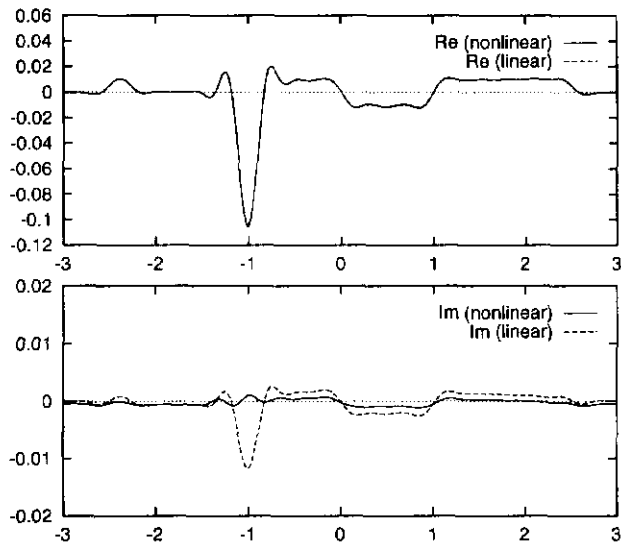


Fig. 4. Linear and nonlinear reconstructions of the inhomogeneity from Figure 3. Upper panel: real parts. Lower panel: imaginary parts.

Images of objects that span larger regions compared to the ultrasonic wavelength are presented in Figure 5. These images were obtained using the modified eigenfunction reconstruction formula of Equation 9, using a 128×128 scattering matrix, 10 eigenfunctions for the five-wire object, and 64 eigenfunctions for the cylinder with internal wires. Five frequencies were employed in each case, so that ka for the cylinder ranged between 28 and 42.

The efficiency of the modified eigenfunction algorithm was compared with two established methods for inversion under weak scattering conditions. The first benchmark method investigated was filtered backpropagation, which employs the reconstruction formula [12]–[14]

$$q_B(\mathbf{x}) = \frac{k^2}{8\pi} \iint |\sin(\alpha - \theta)| A(\theta, \alpha) e^{ik\mathbf{x} \cdot (\theta - \alpha)} d\alpha d\theta. \quad (12)$$

The second is direct Fourier inversion, in which the waves-

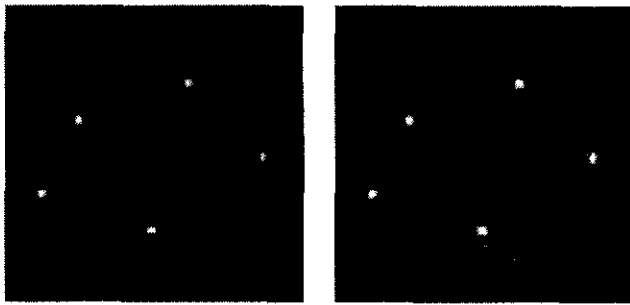


Fig. 5. Real part of reconstructions obtained from computed five-frequency scattering data. Left Panel: five widely-spaced wires. Right Panel: homogeneous cylinder with five internal wires.

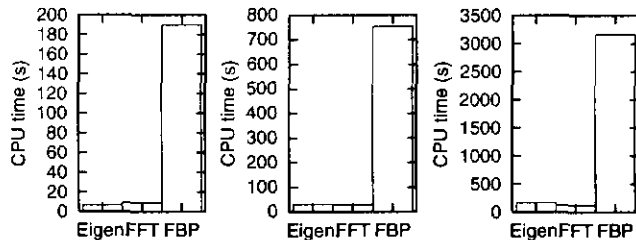


Fig. 6. Comparisons of computation time on a SparcSystem 10 for three inversion methods. Left Panel: 64×64 scattering matrix. Center Panel: 128×128 scattering matrix. Right Panel: 256×256 scattering matrix.

pace representation of the inhomogeneous medium [9]

$$\hat{q}_B[k(\cos \theta - \cos \alpha), k(\sin \theta - \sin \alpha)] = \frac{1}{2\pi} A(\theta, \alpha) \quad (13)$$

is inverted by discrete Fourier transformation after two-dimensional interpolation to uniform grid points in wave-space.

Results of the efficiency comparison are shown in Figure 6. The object employed for these comparisons was the five-wire object shown in Figure 5. Reconstructions were performed using a frequency of 2.5 MHz. Ten eigenfunctions of \hat{A} were employed in the benchmark eigenfunction reconstructions. The results indicate that the modified eigenfunction method, like the original eigenfunction method, is much more efficient than filtered backpropagation. Also, the modified eigenfunction method is seen to be comparably efficient to, and in some cases more efficient than, inversion by fast Fourier transformation.

IV. CONCLUSION

A method for focusing and imaging using scattered acoustic fields has been presented. The method outlined here makes use of the physical properties of scattering operators by using their eigenfunctions as incident-wave patterns.

It has been shown that the eigenfunction method is appropriate for quantitative ultrasonic imaging of large inhomogeneities. In particular, a modified eigenfunction

method allows reconstructions to be performed using a single summation of retransmitted fields. Numerical examples have illustrated this capability.

Comparison of the efficiency of the eigenfunction method to filtered backpropagation and Fourier inversion has been performed. The eigenfunction method is considerably more efficient than filtered backpropagation and is comparable in efficiency to Fourier inversion. When the scattering operator has few eigenvalues, the eigenfunction method can be more efficient than inversion by fast Fourier transformation.

The eigenfunction method has also been employed to derive a nonlinear inverse scattering formula that yields a solution for the scattering potential q in terms of retransmitted fields of eigenfunctions in the scattering medium and in the background medium. This formula has been demonstrated to yield improvement in accuracy and resolution over Born inversion. The method shows potential for future work in iterative nonlinear inverse scattering.

ACKNOWLEDGMENTS

The authors thank Peter Monk for releasing his scattering problem solver under the Gnu Public License and for assistance in the use of his code. Helpful discussions with Petri Ola and Fasil Santosa are acknowledged with pleasure.

REFERENCES

- [1] T. D. Mast, A. I. Nachman, and R. C. Waag, "Focusing and imaging using eigenfunctions of the scattering operator," *J. Acoust. Soc. Am.* **102**, 715–725 (1997).
- [2] D. Isaacson, "Distinguishability of conductivities by electric current computed tomography," *IEEE Trans. Med. Imag.* **MI-5**, 91–95 (1986).
- [3] D. G. Gisser, D. Isaacson, and J. C. Newell, "Electric current computed tomography and eigenvalues," *SIAM J. Appl. Math.* **50**, 1623–1634 (1990).
- [4] O. Ikeda, "An image reconstruction algorithm using phase conjugation for diffraction-limited imaging in an inhomogeneous medium," *J. Acoust. Soc. Am.* **85**, 1602–1606 (1989).
- [5] D. R. Jackson and D. R. Dowling, "Phase conjugation in underwater acoustics," *J. Acoust. Soc. Am.* **89**, 171–181 (1991).
- [6] D. Cassereau and M. Fink, "Time-reversal of ultrasonic fields—Part III: Theory of the closed time-reversal cavity," *IEEE Trans. Ultrason., Ferroelec., and Freq. Control* **39**, 579–592 (1992).
- [7] C. Prada, J.-L. Thomas, and M. Fink, "The iterative time-reversal process: analysis of the convergence," *J. Acoust. Soc. Am.* **97**, 62–71 (1995).
- [8] T. M. Habashy, R. W. Groom, and B. R. Spies, "Beyond the Born and Rytov approximations: a nonlinear approach to electromagnetic scattering," *J. Geophys. Res.* **98**, 1759–1775 (1993).
- [9] P. M. Morse and K. U. Ingard, *Theoretical Acoustics* (New York, McGraw-Hill, 1968), ch. 8.
- [10] D. C. Dobson and F. Santosa, "Resolution and stability analysis of an inverse problem in electrical impedance tomography: dependence on the input current patterns," *SIAM J. Appl. Math.* **54**, 1542–1560 (1994).
- [11] A. Kirsch and P. Monk, "An analysis of the coupling of finite element and Nyström methods in acoustic scattering," *IMA J. Num. Anal.* **14**, 523–544 (1994).
- [12] A. J. Devaney, "A filtered backpropagation algorithm for diffraction tomography," *Ultrason. Imag.* **4**, 336–350 (1982).
- [13] A. J. Devaney and G. Beylkin, "Diffraction tomography using arbitrary transmitter and receiver surfaces," *Ultrason. Imag.* **6**, 181–193 (1984).
- [14] A. Witten, J. Tuggle, and R. C. Waag, "A practical approach to ultrasonic imaging using diffraction tomography," *J. Acoust. Soc. Am.* **83**, 1645–1652 (1988).